Synthesis, Optoelectronic Properties, and Charge Carrier Dynamics of

Colloidal Quasi-two-dimensional Cs₃Bi₂I₉ Perovskite Nanosheets

Sushant Ghimire,*[a] Chris Rehhagen,[a] Saskia Fiedler,[b] Urvi Parekh,[a] Rostyslav Lesyuk,[a,c] Stefan Lochbrunner,[a] Christian Klinke*[a,d,e]

[a.] *Institute of Physics, University of Rostock, Albert-Einstein-Str. 23-24, 18059 Rostock, Germany*

[b.] *Center for Nanophotonics, NWO-Institute AMOLF, Science Park 104, 1098 XG Amsterdam, The Netherlands*

[c.] *Pidstryhach Institute for Applied Problems of Mechanics and Mathematics of NAS of Ukraine, Naukowa str. 3b,79060 Lviv & Department of Photonics, Lviv Polytechnic National University, Bandery str. 12, 79000 Lviv, Ukraine*

[d.] *Department of Chemistry, Swansea University, Swansea SA2 8PP, UK.*

[e.] *Department "Life, Light & Matter", University of Rostock, Albert-Einstein-Strasse 25, 18059 Rostock, Germany.*

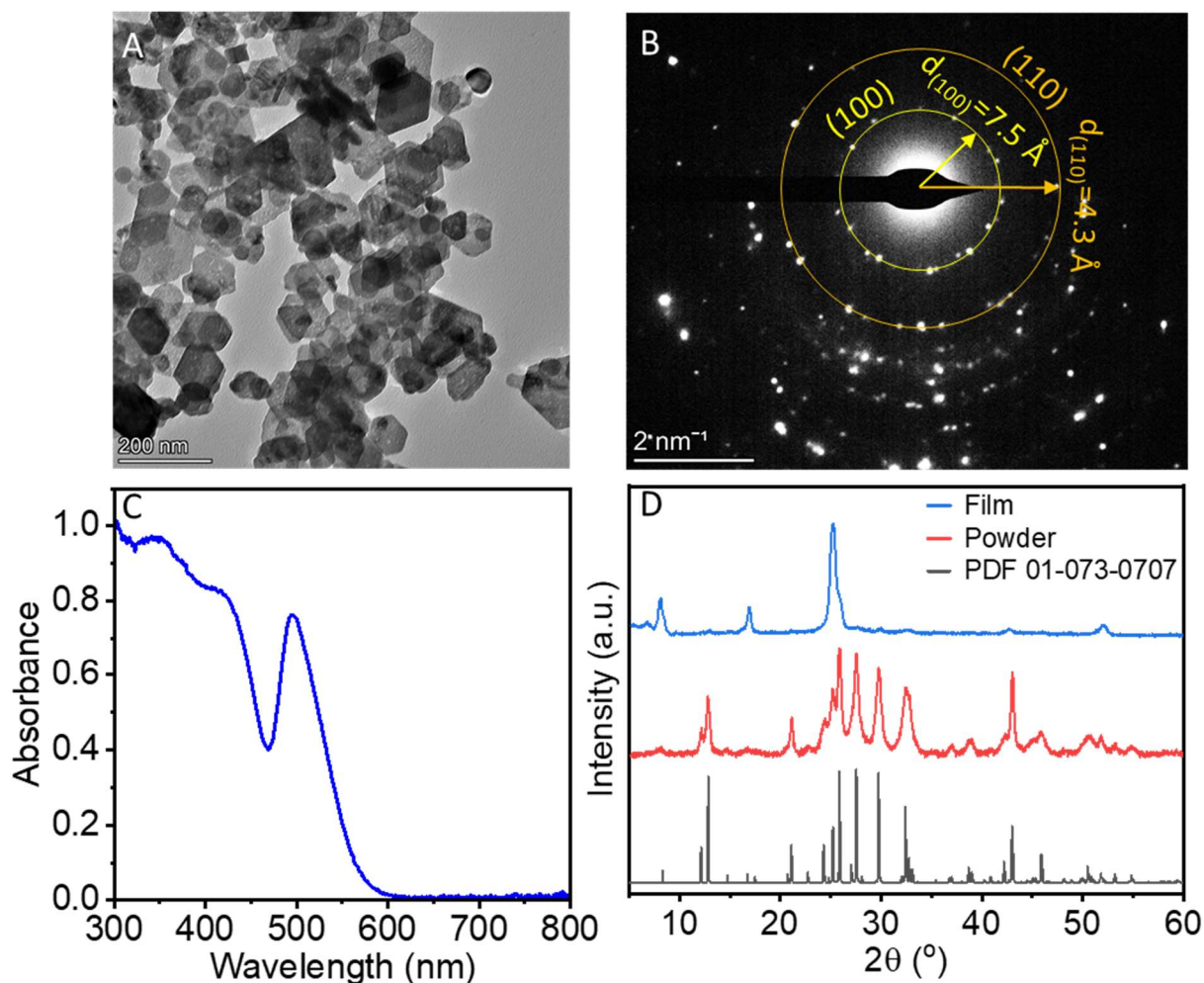*Corresponding authors: sushant.ghimire@rostock.de, christian.klinke@uni-rostock.de

Fig. S1 Characterization of $Cs_3Bi_2I_9$ precipitates obtained from the hot-injection method. (A) Transmission electron microscope (TEM) image of nanoplates. (B) Selected area electron diffraction (SAED) of the nanoplates showing ring pattern. (C) UV-vis absorption spectrum of the sample dispersed in toluene. (D) X-ray diffraction pattern of the film and powder of the precipitate compared with Powder Diffraction File (PDF) card number 01-073-0707.
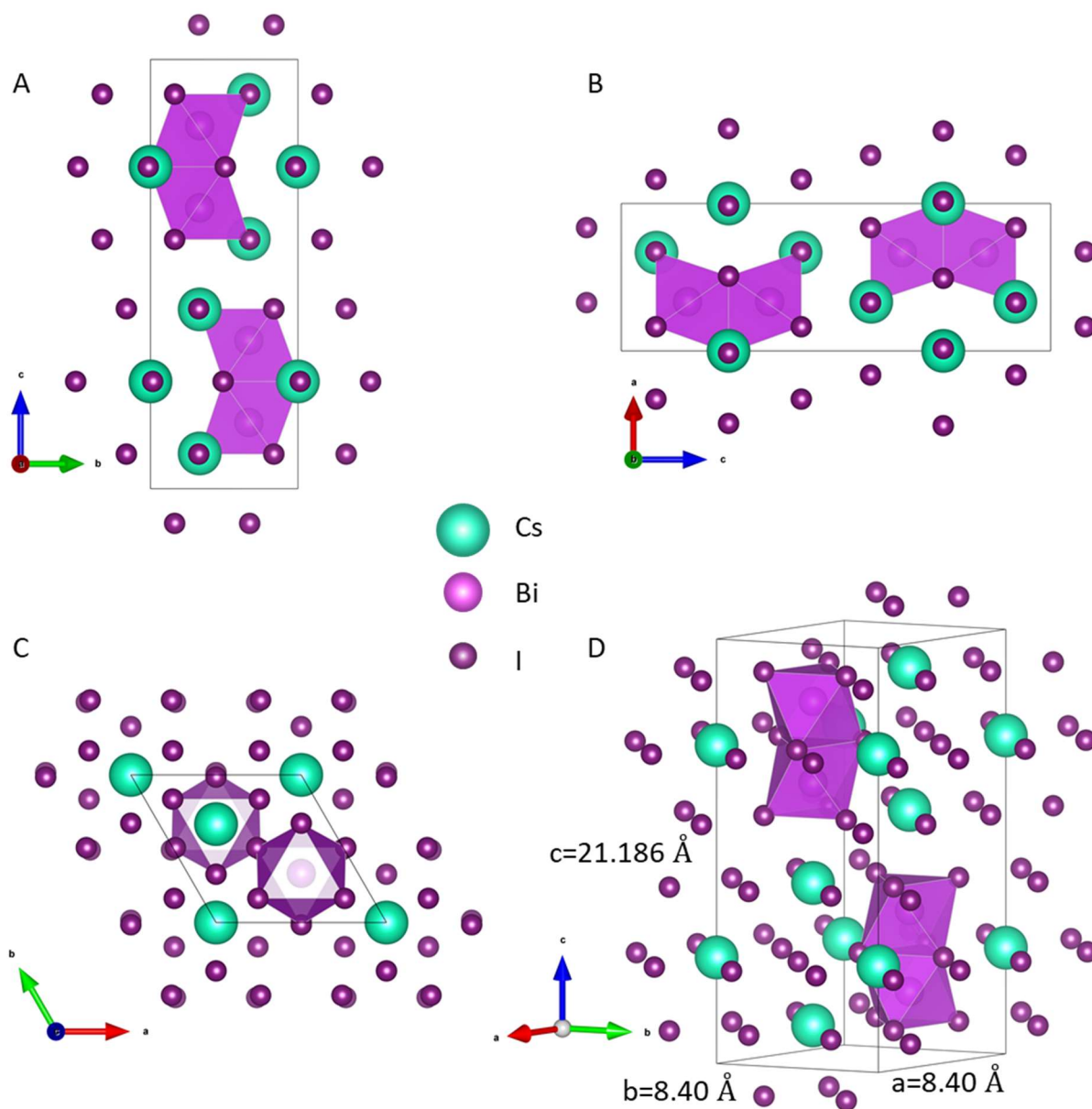
The TEM image in Fig. S1 (A) shows the size distribution of small and large nanoplates. The corresponding SAED pattern [Fig. S1 (B)] shows rings, indicating the polycrystalline nature of the sample. We calculated the d-spacings from the ring patterns in SAED as 7.5 Å and 4.3 Å and assigned the corresponding rings as the diffraction spots from (100) and (110) planes, respectively of a hexagonal crystal structure. The XRD patterns in the film and powder form of $Cs_3Bi_2I_9$ precipitates are shown in Fig. S1 (D) and compared with the standard XRD patterns obtained from the PDF card number 01-073-0707. Although the $Cs_3Bi_2I_9$ precipitates show lateral size distribution, their UV-visible absorption spectrum is comparable with that (see Fig. 4A in the main text) of large quasi-2D $Cs_3Bi_2I_9$ nanosheets obtained from the selective reprecipitation. This is obvious since the confinement of excitons happens within the 0D molecular structure [i.e. the isolated $(Bi_2I_9)^{3-}$ dimers] which is present in $Cs_3Bi_2I_9$ perovskites irrespective of their lateral size and shape.[1,2]
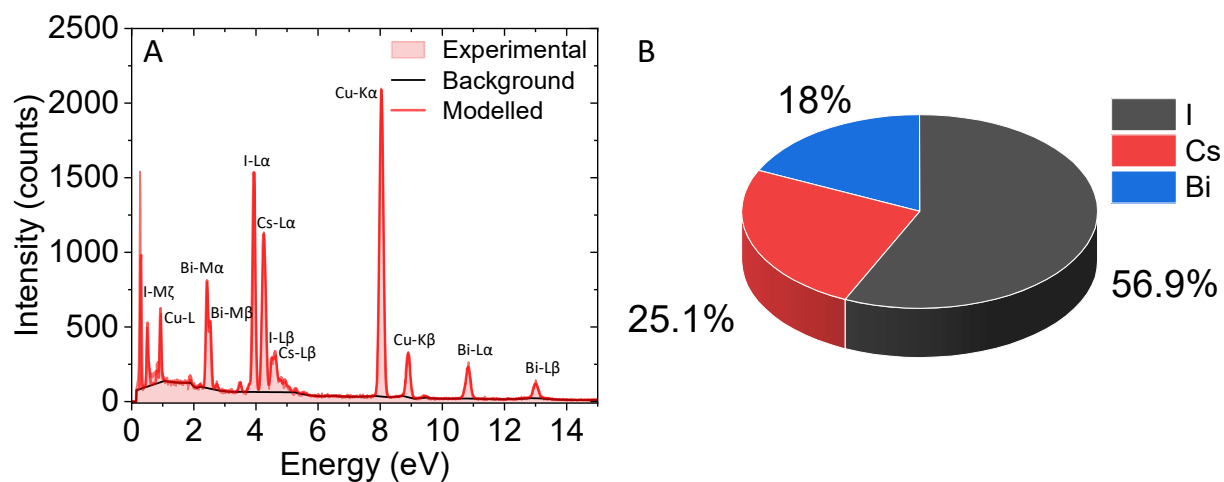
Fig. S2 (A) Energy dispersive X-ray (EDX) spectrum of a quasi-2D $Cs_3Bi_2I_9$ nanosheet. (B) Elemental composition with atomic fractions of constituent elements in percentage obtained from the EDX spectrum.

Table S1: List of powder XRD peaks and the corresponding d-spacings of Cs3Bi2I9 nanosheets at different 2θ angles that are assigned to different *hkl*. Lattice parameters (a=b, and c) are calculated using $d_{(100)}$ and $d_{(006)}$, respectively.

| (*hkl*)	2θ	d-spacing (Å)	a (Å)	b (Å)	c (Å)
002	8.351	10.579			
100	12.146	7.280			
101	12.831	6.890			
004	16.732	5.294			
104	20.696	4.288			
110	21.094	4.208			
112	22.725	3.909			
200	24.418	3.642			
006	25.201	3.531			
202	25.830	3.446			
203	27.516	3.239	8.40	8.40	21.186
204	29.722	3.003			
205	32.366	2.764			
300	36.965	2.430			
300	37.066	2.423			
0010	42.611	2.120			
0010	42.717	2.115			
305	42.934	2.105			
209	45.826	1.978			
0012	51.696	1.767			
403	51.834	1.762			

Fig. S3 Unit cell crystal structure of quasi-2D $Cs_3Bi_2I_9$ nanosheets at different orientations modeled using the lattice parameter values calculated from the experimental powder XRD data provided in Table S1. The drawings were produced using VESTA software.[3]
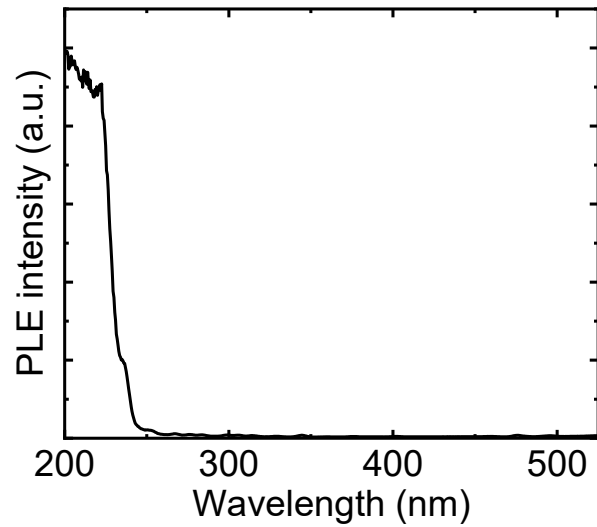
Fig. S4 Photoluminescence excitation (PLE) spectrum of quasi-2D Cs₃Bi₂I₉ nanosheets.
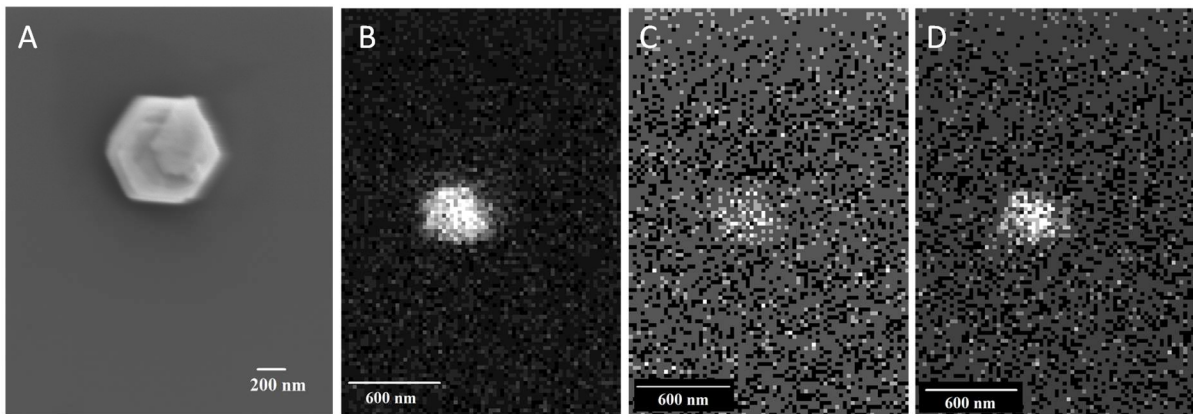
Fig. S5 (A) Scanning electron microscope (SEM) image of quasi-2D Cs₃Bi₂I₉ nanosheets. (B-D) Panchromatic cathodoluminescence (CL) maps of the nanosheets (B) without filter, (C) with 500/50 nm bandpass filter, and (D) 600/50 nm bandpass filter.

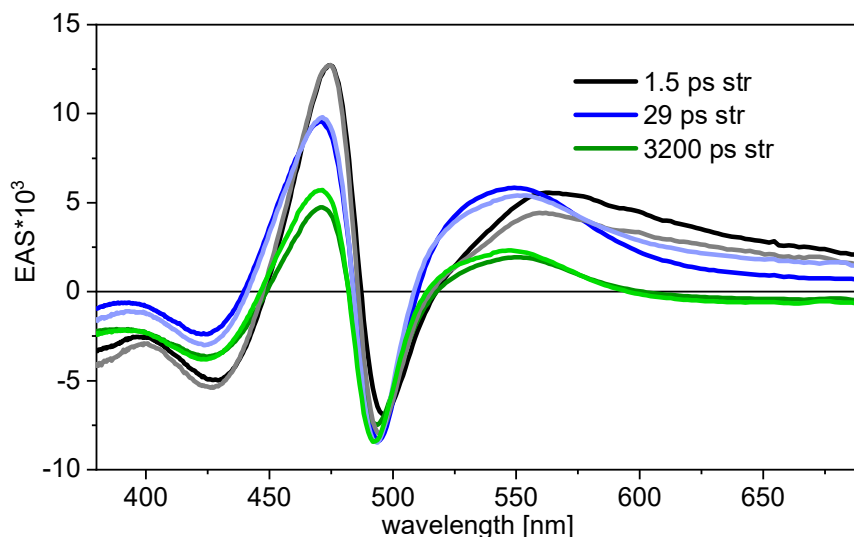*Fitting of transient absorption data*

For fitting the transient absorption data, the coupled differential equations for the sequential model with three stretched exponentials read as follows:

$$\frac{dn_1}{dt} = -\frac{n_1}{2\sqrt{t \cdot \tau_1}} \qquad n_1(0) = 1$$

$$\frac{dn_2}{dt} = +\frac{n_1}{2\sqrt{t \cdot \tau_1}} - \frac{n_2}{2\sqrt{t \cdot \tau_2}} \qquad n_2(0) = 0$$

$$\frac{dn_3}{dt} = +\frac{n_2}{2\sqrt{t \cdot \tau_2}} - \frac{n_3}{2\sqrt{t \cdot \tau_3}} \qquad n_3(0) = 0$$

The population of the species n_1, n_2, and n_3 decayed sequentially starting with the complete population in n_1. The time constants τ are freely fitted parameters. The data is fitted globally with the equation:

$$TA(\lambda, t) = EAS_1(\lambda) \cdot n_1(t) + EAS_2(\lambda) \cdot n_2(t) + EAS_3(\lambda) \cdot n_3(t)$$

The values of each evolution-associated spectra (EAS) at a certain probe wavelength thus correspond to the amplitudes of the related species, where the time constants are fitted globally.

Fig. S6 EAS obtained from the global fitting of the transient absorption spectra with three stretched exponential decay functions of colloidal quasi-2D Cs$_3$Bi$_2$I$_9$ nanosheet solutions in toluene excited with a photon energy of 2.48 eV and at different excitation intensities. The lines with dark colors show the EAS at 200 µW excitation power and the light-colored curves with 60 µW. The time constants are determined with the 200 µW data and set as constant for 60 µW. The EAS of the 60 µW data is multiplied by 3.33 corresponding to 200µW/60µW.
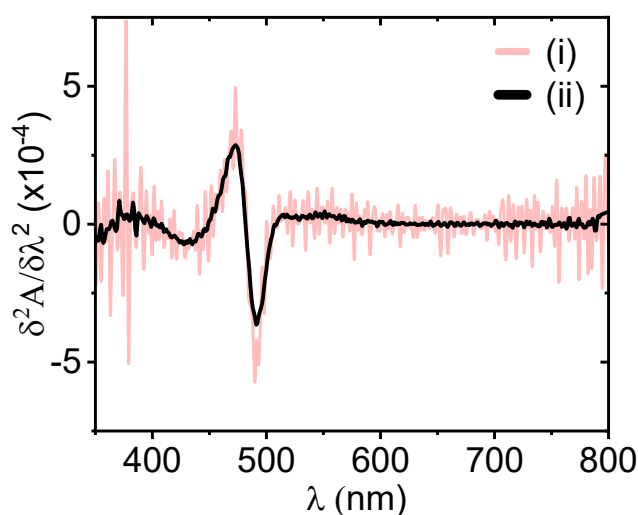
Fig. S7 Second derivative spectrum of the steady-state absorption spectrum, which is shown in Fig. 4A in the main text. (i) Raw data and (ii) smoothed plot.

Notes and references

1 F. Bai, Y. Hu, Y. Hu, T. Qiu, X. Miao and S. Zhang, *Sol. Energy Mater. Sol. Cells*, 2018, **184**, 15–21.

2 Y. Zhang, Y. Liu, Z. Xu, H. Ye, Z. Yang, J. You, M. Liu, Y. He, M. G. Kanatzidis and S. (Frank) Liu, *Nat. Commun.*, 2020, **11**, 2304.
3 K. Momma and F. Izumi, *J. Appl. Crystallogr.*, 2011, **44**, 1272-1276.